University of California, San Diego UCSD-ENG-089

Improved Performance of Energy Recovery Ventilators Using Advanced Porous Heat Transfer Media

M. S. Tillack, A. R. Raffray and J. E. Pulsifer

December 2001

Fusion Division
Center for Energy Research

University of California, San Diego
La Jolla, CA 92093-0417

Table of Contents

List of Figures

List of Tables

Abstract

Energy recovery ventilators (ERV's) use air-to-air heat exchangers to retain building heat (or cold) while allowing fresh air exchange. As buildings become more leak-tight, improved efficiency for energy recovery ventilators will continue to grow in importance. Improvements in heat transfer effectiveness, without commensurate increase in capital and operating cost, would enable this important energy saving technology to play a larger role in improving building energy efficiency in California.

The overall objective of this research was to demonstrate through design, numerical modeling and experiments that the heat transfer effectiveness of energy recovery ventilators could be increased beyond current standards of 50-70% with acceptable cost and reliability by using advanced porous heat transfer media.

Modeling tools were developed for random and oriented fiber geometries. The models were used to estimate thermal hydraulic performance. Relatively short heat exchangers with very high porosity (order of 98-99%) were found to be optimum. One of the candidate materials tested – an ESLI carbon velvet – is predicted to offer superior effectiveness for a given pumping power. For 99.5% porosity, models predict an achievable effectiveness of 90% with pumping power below 5% of the heat recovered.

Relevant thermal-hydraulic conditions were simulated in our experimental apparatus. Measured pressure drops were lower than model predictions, suggesting flow bypass was occurring. Flow bypass can occur if the packing density is nonuniform or if the porous medium loses contact with the walls. Heat transfer performance was also degraded. For the ESLI fiber, models predict effectiveness over 95%, whereas the measured value was 77%. Further work will be needed to resolve these discrepancies.

Key Words: *porous media, energy recovery ventilators, recuperator effectiveness*

Executive Summary

Energy recovery ventilators use air-to-air heat exchangers to retain building heat (or cold) while allowing fresh air exchange. Several manufacturers already supply products which can be used in either commercial or residential buildings, for either central or window-mounted applications. The heart of the system is the heat exchanger, which in some cases is used also to aid in filtration and/or humidity control. Using forced convection (*i.e.,* fans), typical heat exchanger efficiencies may be as high as 70–80%, but values as low as 50% have been observed (the efficiency is defined as the ratio of energy transferred between the two air streams compared with the total energy transported through the heat exchanger). With such low efficiencies, the capital and maintenance costs of the additional heat exchanger system might not be recovered for many years, if ever. Substantial improvements in heat transfer efficiency are possible using modern low-cost gas-phase heat exchanger technology. We believe that heat exchanger effectiveness in excess of 90% is possible using high conductivity porous media. Increasing the heat transfer effectiveness to 90% would provide a substantial improvement in energy loss.

In this project, we explored improvements in energy recovery effectiveness that are possible with porous heat transfer media. Design and operating parameters were established in order to assure relevance of the models and experimental data. Two modeling approaches were used in order to estimate the pressure drop and heat transfer coefficient in high-porosity materials:

(1) Effective thermal and fluid properties were calculated from first principles using semi-empirical data, and

(2) A 2D porous media heat transfer model called MERLOT was developed and applied to this problem.

Various types of fibrous heat transfer media were obtained and fabricated into small test articles for testing. A test rig was assembled with computer-controlled flow and heating rates, and data were collected for pressure drop and overall heat transfer coefficient between the hot and cold streams (Section 4.3). Finally, the test results were compared with models of heat transfer in porous media in order to verify the performance and to help identify any sources of discrepancies.

The following outcomes were obtained:

1. Outcome of initial assessment. Preliminary analysis showed that thermal-hydraulic conditions expected in buildings could be obtained easily in our experimental apparatus. Relatively short heat exchangers with high porosity (order of 98-99%) were found to be optimum. Based on initial estimates, a heat exchanger effectiveness of 90% appeared feasible.

2. Outcome of modeling. Modeling tools were developed for random and oriented fiber geometries. The models then were used to estimate thermal hydraulic performance. For the high porosity cases examined (>99%), the carbon velvet exhibits superior thermal performance, albeit at a higher pressure drop penalty. Due to the high porosity and oriented architecture, very simple models can be used to predict and optimize the performance of fiber-flocked heat exchangers. Using these models, extensive parametric studies were performed. For 99.5% porosity, models predict an achievable effectiveness of 90% with pumping power only 5% of the heat recovered and a heat exchanger length of 7 cm.

3. Outcome of experimental verification. Experiments were performed on open channels, metal wools and carbon velvet. Effectiveness in open channels agreed well with predictions, but the performance with porous media in the channels were consistently lower than expected. Flow bypass was a recurring problem, especially at higher velocities. Local and/or global flow redistribution could reduce both the pressure drop and heat transfer coefficient, consistent with observations. Measurements of the ratio of pumping power to thermal power removed actually agree well with predictions, supporting these observations.

Numerical modeling indicates that the optimum performance of porous media heat exchangers occurs with fiber diameters above about 10 μm and porosity in the range of 98-99%. In this range, effectiveness over 90% is predicted while maintaining pumping power within reasonable limits. Both random and oriented fiber geometries appear to offer adequate performance. Experimental studies were unable to replicate the high performance predicted by numerical modeling. Since both pressure drop and heat transfer coefficient were depressed, the most likely explanation for the discrepancies is the existence of flow bypass.

Two primary improvements are recommended in order to further explore the potential of carbon velvet porous media. First, extensive parametric studies indicated that the choice of parameters for the materials used in the experiments were not optimum. In order to achieve higher effectivness, slightly larger fiber diameters with porosity of 99% (instead of 99.5%) should be used. In addition, fibers with conductivity about a factor of two higher (200 W/m-K), which is relatively straightforward and carries little cost penalty, should be used. Second, greater care should be

taken to assure that the fibers are well attached to the walls in order to prevent flow bypass. This is actually rather simple to do by interlocking velvets which are bonded to both sides of the coolant channels.

Model predictions suggest that metallic wools could offer equal or better performance as compared with carbon velvets if sufficiently high conductivity materials, such as copper, could be obtained with appropriate dimensions and packing characteristics. Further exploration of low-cost sources of high-porosity, high-conductivity metal fillers is needed.

Successful development of high-effectiveness heat exchangers will expedite the application of energy recovery ventilators in California. For a well-sealed house, assuming an electricity cost of $0.10/kWh, an energy recovery ventilation system with a 90% effectiveness and a duty factor of about 45% would result in a utility cost saving of about $400 per year.

1. Introduction

The current trend toward sealing houses to reduce air and moisture infiltration makes them more energy efficient and reduces home energy costs. Depending on the local climate, appliance use and sealing method, tighter houses can be 15% to 30% more energy efficient, often saving several hundred dollars per year in energy costs. However, as homes and commercial buildings become more leak tight, adequate ventilation becomes increasingly important in order to avoid air quality problems. If a house is constructed tighter than 0.35 air changes per hour (ACH), pollutants generated in the home can accumulate and reduce the indoor air quality to unhealthy levels. If fresh outside air is brought in through an open window to alleviate this problem, this air may be excessively hot, cold or humidity-laden and require conditioning at added expense.

Energy recovery ventilators (ERV's) use air-to-air heat exchangers to retain building heat (or cold) while allowing fresh air exchange. Several manufacturers already supply products which can be used in either commercial or residential buildings, for either central or window-mounted applications. The heart of the system is the heat exchanger, which in some cases is used also to aid in filtration and/or humidity control. Using forced convection (*i.e.*, fans), typical heat exchanger efficiencies may be as high as 70–80% [1], but values as low as 50% have been observed [2] (the efficiency is defined as the ratio of energy transferred between the two air streams compared with the total energy transported through the heat exchanger). With such low efficiencies, the capital and maintenance costs of the additional heat exchanger system might not be recovered for many years, if ever.

During recent years, energy recovery ventilators have increased in popularity throughout the world. However, their implementation in California has lagged, partly due to relatively poor heat exchanger effectiveness which leads to longer energy payback times. As buildings become more leak-tight, improved efficiency for energy recovery ventilators will continue to grow in importance. Improvements in heat transfer effectiveness, without commensurate increase in overall unit cost, would enable this important energy saving technology to play a larger role in improving building energy efficiency in California.

Substantial improvements in heat transfer efficiency are possible using modern low-cost gas-phase heat exchanger technology. We believe that heat exchanger effectiveness in excess of 90% is possible using high conductivity porous media. Increasing the heat transfer effectiveness to 90% would provide a factor of 2–5 improvement in energy loss.

In this project, we explored improvements in energy recovery effectiveness that are possible with innovative heat transfer media. Design and operating parameters were established in order to ensure relevance of the models and experimental data (Section 4.1). Two modeling approaches were used in order to estimate the pressure drop and heat transfer coefficient in high-porosity materials (Section 4.2):

(1) Effective thermal and fluid properties were calculated from first principles using semi-empirical data, and

(2) A 2D porous media flow model called MERLOT was developed and applied to this problem.

Various types of fibrous heat transfer media were obtained and fabricated into small test articles for testing. A test rig was assembled with computer-controlled flow and heating rates, and data were collected for pressure drop and overall heat transfer coefficient between the hot and cold streams (Section 4.3). Finally, the test results were compared with models of heat transfer in porous media in order to verify the performance and to help identify any sources of discrepancies.

2. Project Objectives

The overall objective of this research was to demonstrate through design, numerical modeling and experiments that the heat transfer effectiveness of energy recovery ventilators can be increased beyond current standards of 50-70% with acceptable cost and reliability by using advanced porous heat transfer media. Related project objectives were to:

- Determine testing parameters which correctly simulate the application. Perform parametric analyses in order to optimize the heat transfer medium.
- Develop modeling tools that are applicable to very high porosity media. This is a regime with little data and no general models that accurately predict heat transfer coefficient.
- Measure pressure drop and heat transfer coefficient in order to verify the model predictions and to provide direct demonstration of system performance.

3. Project Approach

Four primary tasks were performed in this project: 1. An initial design assessment, 2. Model development and parametric studies, 3. Experimental setup and testing, and 4. Final assessment.

Task 1: Design assessment. We began by developing the basic heat exchanger design, including nominal geometric and flow parameters. A range of material geometries and compositions were explored in order to determine the optimum characteristics of the heat transfer medium, and to determine which technique is most suitable for this application. Three classes of porous media were considered: (1) metal wools with cylindrical or rectangular cross section, (2) porous foams made of metal or carbon, and (3) carbon fiber velvet. Detailed designs of the test articles were prepared.

Task 2: Modeling and parametric studies. Both the heat transfer coefficient and the pressure drop were studied so that thermal efficiency and pumping power could be determined and optimized. Three modeling subtasks were performed:

1. Each microstructure was assessed to determine the most appropriate modeling approach for both pressure drop and heat transfer coefficient. These models range from simple semi-empirical formulas to more complex multi-dimensional numerical models.
2. Detailed models were developed. An independent fiber model was used for high-porosity oriented structures (such as the ESLI carbon velvet). A 2D code called MERLOT was developed for modeling heat transfer in porous metal wools.
3. Parametric studies were performed to determine optimum performance conditions. Key variables include porosity, surface area density, thermophysical properties and flow conditions.

Task 3: Experiment setup and testing. Potential suppliers were contacted to determine the availability of sample materials and material optimization studies were undertaken. The heat transfer media were integrated into the test articles. A data acquisition system was assembled and instrumentation was installed into the test articles. All instrumentation and controls (including heater and fan power supplies) were connected to the computer data acquisition

system running Labview™. Electrical resistance heaters were used to control the temperature of the hot stream. The effectiveness and heat transfer coefficient were obtained simply by measuring the inlet and outlet temperatures. The pressure drop was measured with a differential pressure gage and the gas flow rate with a hand-held impeller-type flow meter.

Task 4: Final assessment. Experimental results were compared with model estimates and discrepancies were examined. The results were used to determine the ability of various regenerator core designs to provide improvements over existing ERV designs and to provide recommendations on further R&D needs.

4. Project Outcomes

4.1 Design parameters and porous media options

Outcome: ***Preliminary analysis showed that t****hermal-hydraulic conditions expected in buildings could be obtained easily in our experimental apparatus. Relatively short heat exchangers with very high porosity (order of 98-99%) were found to be optimum. Based on initial estimates, heat exchanger effectiveness of 90% appeared feasible.*

Initial scoping of the heat exchanger configuration and parameter ranges was performed in order to ensure that modeling and experiments would be relevant to the problem of residential heating and cooling. Table 1 summarizes parameters for a prototypical house with 2000 sq. ft. and 0.35 ACH (air changes per hour) requirement. Simulation parameters used in our test assembly are also shown. The geometry of a prototypical heat exchanger is shown in Figure 1, and all parameters are defined in the Nomenclature.

Table 1. Thermal-hydraulic parameters for a prototypical home and the test article

	W CFM	**d** inches	**t** inches	**D** inches	**Re_d**	**T_{in}** ^0C	**T_{out}** ^0C	**q_{max}** Watts
2000 sq ft Home:	117	10.5	1/8	15	1.8×10^4	20	-10	2035
Test Article:	4 to 20	1.936	0.032	3.068	$3.3\text{-}17 \times 10^3$	20	-10	70 to 350

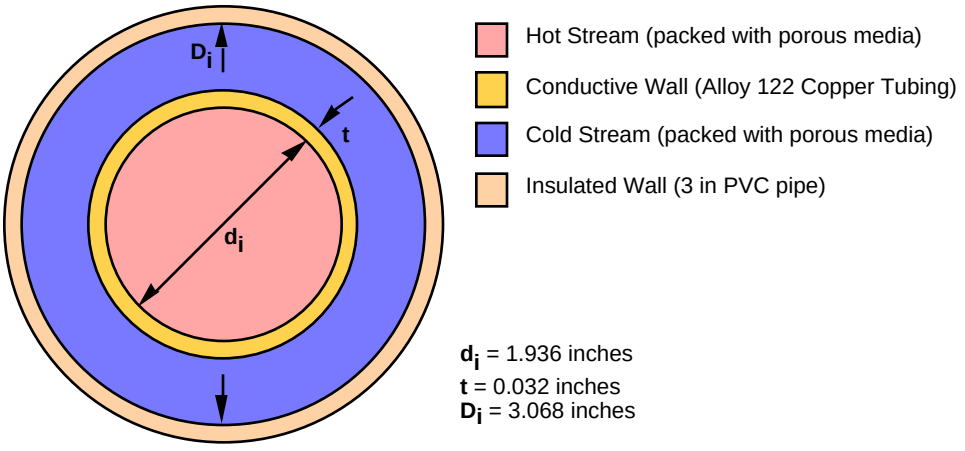

Figure 1. Cross section of a prototypical coaxial heat exchanger

A range of material geometries and compositions were explored in order to determine the optimum characteristics of the heat transfer medium. Three classes of porous media were considered (see Figure 2): (1) metal wools with cylindrical or rectangular cross section, (2) porous foams made of metal or carbon, and (3) carbon fiber velvet.

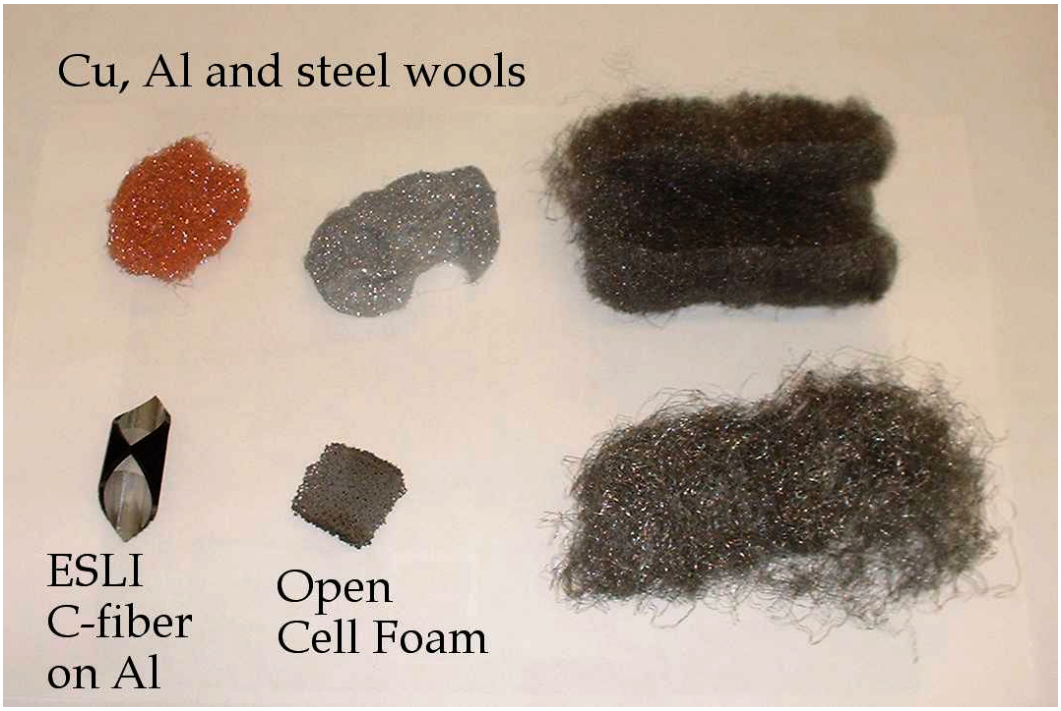

Figure 2. Example of thermal media (ESLI carbon fibers, metal wools, open-cell foam, tailings)

Thermofluid performance of the various options was explored numerically. A model called MERLOT (see Section 4.2.4) was developed to estimate the effective heat transfer coefficient for metal wools. An "independent fiber model" (see Section 4.2.3) was used to calculate the values for the ESLI velvet. For each case, the heat exchanger effectiveness was set to 90% (our goal) and then the resulting heat transfer coefficient, length and pressure drop were calculated.

Table 2 summarizes the results. All cases were assumed to have 117 cfm with velocity of 1 m/s (the flow area is 0.0552 m^2 for all cases, assuming an inside pipe diameter of 0.265 m). The empty pipe case effectively demonstrates the limitations of a simple open heat exchanger. In order to obtain effectiveness of 90%, the heat exchanger must be very long.

Table 2. Performance comparison of heat transfer options for a prototypical home with required effectiveness of 90%

ϕ	dP/dx (Pa/m)	L_x (m)	ΔP (Pa)	h (W/m^2K)
No media				
100%	0.061	292	17.8	4.8
Copper (400 W/m-K, 100 μm)				
98%	1,440	3.15	4,536	450
95%	4,231	1.33	5,627	1,068
90%	11,042	0.77	8,502	1,832
Steel (25 W/m-K, 100 μm)				
90%	11,042	7.23	79,834	195
ESLI fibers (100 W/m-K, 6 μm)				
99%	256,826	1.3	68,059	1,056
98%	314,679	0.62	83,390	2,108

The fiber diameter assumed for the metal wools was 100 μm (as measured from various samples). Results for copper wool of various porosities demonstrates the trade-off between pressure drop and length for porous fillers. Increasing porosity decreases both the pressure drop and heat transfer coefficient. The optimum balance of low pressure drop with acceptable heat transfer occurs at relatively high values of porosity (see Section 4.2). Steel wool was examined as an alternative; it shows that high solid-phase conductivity is very important to obtain good performance. The much lower effective heat transfer coefficient requires a much longer heat exchange in order to obtain 90% effectiveness.

The diameter of the ESLI fibers was assumed to be 6 μm (as measured). Thermal performance was modeled with the independent fiber model presented in Section 4.2.3 while pressure drop was calculated using the Darcy formulated model (Jackson and James) presented in Section 4.2.3. For the same velocity and flow rate, the pressure gradient is much higher for the carbon velvet due to the much smaller diameter. The heat exchanger length is somewhat shorter and the heat transfer coefficient is somewhat improved at similar porosity. Achieving optimum performance requires tailoring of several parameters. Section 4.2.5 details parametric studies for the carbon velvet.

Additional analysis was performed for the carbon velvet in order to determine a set of parameters for experimentation. A goal heat exchanger effectiveness was chosen and then the pressure drops for various porosities and associated lengths were compared (see Table 3). Interestingly, the model shows that the pressure drop is nearly independent of porosity for a fixed effectiveness.

Table 3. Assessment of ESLI carbon velvet based on pin fin model (90% effectiveness, V=0.5 m/s, D_{fiber}=6 μm, k_{fiber}=100 W/m-K)

Porosity	U (W/m^2-K)	L (m)	Pressure Drop (Pa)
0.999	202	0.109	119
0.998	396	0.055	121
0.997	591	0.037	122
0.996	785	0.028	122
0.995	980	0.022	123
0.994	1,174	0.019	123
0.993	1,369	0.016	123
0.992	1,563	0.014	123
0.991	1,758	0.012	123
0.990	1,952	0.011	123

(U is overall heat transfer coefficient, L is heat exchanger length)

Table 4. Assessment of ESLI carbon velvet based on pin fin model (95% effectiveness, V=0.5 m/s, D_{fiber}=6 μm, k_{fiber}=100 W/m-K)

Porosity	U (W/m^2-K)	L (m)	Pressure Drop (Pa)
0.999	202	0.230	252
0.998	396	0.117	256
0.997	591	0.078	258
0.996	785	0.059	259
0.995	980	0.047	259
0.994	1,174	0.039	259
0.993	1,369	0.034	260
0.992	1,563	0.030	260
0.991	1,758	0.026	260
0.990	1,952	0.024	260

(U is overall heat transfer coefficient, L is heat exchanger length)

As porosity decreases, the length necessary to achieve a given effectiveness also decreases. In the limit of high porosity, the length and porosity can be traded off; the total number of "pin fins" is the parameter which dominates thermal-hydraulic performance. Porosities less than 99% require very little exchanger length to achieve 90% effectiveness. A case with 95% effectiveness was explored in order to determine whether higher performance might be possible (see Table 4).

The pressure drop and effective heat transfer coefficient were calculated for four different air velocities for a heat exchanger effectiveness of 90% and 95%. Table 5 shows the results. Experimentally, we were not able to achieve 5 m/s due to the high pressure drop. In order to obtain reasonably low pumping power with adequate thermal performance, we chose to fabricate two test articles – one with 7 cm length and one with 25 cm length. In both cases the porosity was chosen to be ~99.55% in order to maintain low pumping power.

Table 5. Pressure drop and effective heat transfer coefficient for 99.6% porous ESLI carbon velvet based on pin fin model predictions

ε	V (m/s)	U (W/m^{2}K)	L (m)	ΔP (Pa)	Q (W)
0.95	0.5	785	0.059	259	10
	1	849	0.109	1,112	21
	3	990	0.281	10,724	63
	5	1,077	0.430	32,765	104
0.90	0.5	785	0.028	122	10
	1	849	0.052	527	20
	3	990	0.133	5,080	59
	5	1,077	0.204	15,520	99

The reference application of a 2,000 square foot home and 0.35 air changes per hour requires 1,390 W of heat transferred for a temperature difference of 20 ˚C between the inside and outside of the home. The last column (Q) in Table 5 demonstrates that the ESLI test article would transfer 21 W for a velocity of 1 m/s and a 20˚C temperature difference using 0.055 m^2 of double-sided carbon fiber carpet. Scaling to a household application, less than 4 m^2 of ESLI material would be needed to construct a full heat exchanger to accommodate 1,390 W at 1 m/s velocity. The carpet could be arranged in flat layers to make a very compact heat exchanger with volume of the order of a few cubic feet.

4.2 Numerical modeling and parametric studies

Outcome: *Modeling tools were developed for random and oriented fiber geometries. The models then were used to estimate thermal hydraulic performance. For the high porosity cases examined (>99%), the carbon velvet exhibits superior thermal performance, albeit at a higher pressure drop penalty. Due to the high porosity and oriented architecture, very simple models can be used to predict and optimize the performance of fiber-flocked heat exchangers. Using these models, extensive parametric studies were performed. For 99.5% porosity, models predict an achievable effectiveness of 90% with pumping power only 5% of the heat recovered and a heat exchanger length of 7 cm.*

Two modeling approaches were used in order to estimate the pressure drop and heat transfer in high-porosity materials: (1) effective thermal and fluid properties were calculated from first principles using semi-empirical data, and (2) a 2D porous media flow model called MERLOT was developed and applied to this problem. Detailed parametric studies were performed for the carbon velvet by varying the porosity, flow velocity, fiber conductivity and diameter.

4.2.1 Heat transfer relations

Heat exchanger effectiveness, ε, is the ratio of the actual heat transferred to the maximum possible heat that could be transferred in an infinitely long counter-flow heat exchanger:

$$\varepsilon = \frac{\dot{Q}}{\dot{Q}_{\max}} = \frac{C_H(T_{H,in} - T_{H,out})}{C_{\min}(T_{H,in} - T_{C,in})} = \frac{C_C(T_{C,out} - T_{C,in})}{C_{\min}(T_{H,in} - T_{C,in})}$$

C_C is the flow thermal capacity of the cold stream, C_H is the flow thermal capacity of the hot stream, and C_{min} is the minimum of C_H and C_C.

$$C = \dot{m} c_p$$

For a balanced flow heat exchanger, where hot and cold streams have nearly equal flow thermal capacity, C_H=C_C, the effectiveness simplifies to:

$$\varepsilon = \frac{\dot{Q}}{\dot{Q}_{\max}} = \frac{(T_{H,in} - T_{H,out})}{(T_{H,in} - T_{C,in})} = \frac{(T_{C,out} - T_{C,in})}{(T_{H,in} - T_{C,in})}$$

The prediction of heat transfer performance for a heat exchanger is usually calculated using the number of transfer unit (NTU's), represented by the following expression for a balanced counter-flow heat exchanger:

$$NTU = \frac{UPL}{\dot{m} c_p}$$

where

U is the overall heat transfer coefficient between the two streams
P is the perimeter of the heat transfer interface
L is the length of the heat exchanger
$\dot{m}$ is the mass flow of the working fluid (air)
c_p is the specific heat of the working fluid (air)

The effectiveness is related to the number of transfer units according to the following:

$$\varepsilon = \frac{NTU}{1 + NTU}$$

The geometry of the test article determines P and L. The mass flow is chosen, and the specific heat capacity for air is a known property. The only value that needs to be computed is U. The general formula for U includes all resistances between the two flow streams (including for example the conduction in the interface material):

$$U = \frac{1}{\left(\frac{2A_{cell}}{h_{wall} A_{wall} + h_{fiber,eff} A_{fiber}} + \frac{t}{k_{Al}} \right)}$$

In all cases we examined, the dominant term is the effective heat transfer coefficient on one side of the heat exchanger, h_{eff}. In this case, $U = h_{eff}/2$.

4.2.2 Open channel analysis

For the open channel (100% porous) case, the heat transfer coefficient, h, is simply:

$$h = \mathrm{Nu}_d \left(\frac{k}{d} \right)$$

We can use the familiar Dittus-Boelter relation to determine the Nusselt number:

$$\mathrm{Nu} = 0.023\mathrm{Re}^{0.8}\,\mathrm{Pr}^{0.4}$$

For example, the 25-cm long test article with 100% porosity and 20 CFM flow rate has h = 20 W/m-K in the hot stream. Assuming the same h in the cold stream annulus, the predicted effectiveness is only 4.1%. For the oriented fiber and metal wool cases, a more detailed treatment of the heat transfer coefficient is needed.

4.2.3 Pin fin analysis of ESLI fibers (the "independent fiber model")

We approximated the ESLI carbon velvet as a series of independent pin fins for the purpose of thermal and fluid-dynamic calculations. The fibers of the carbon velvet are, on average, 9 fiber diameters apart for 99% porosity and are almost 13 fiber diameters apart for 99.5% porosity. The local effects of pressure drop and heat transfer coefficient on one fiber are summed over the total number of fibers in the flow path to arrive at the total pressure drop and overall heat transfer coefficient.

Pressure drop calculation

Pressure drop due to viscous shear at the walls of the flow path was found to be negligible as compared to the pressure drop due to the fibers themselves, even at high porosity. Therefore, the only component of pressure drop included in our model is due to drag over the fibers. A cylinder oriented perpendicular to the flow is used to model the drag force on one fiber:

$$F = C_D \frac{1}{2} \rho V^2 L_{cyl} d_{cyl}$$

Flow velocities between 0.5 m/s and 1 m/s result in Reynolds number between 0.3 and 0.7 for external air flow over a 10 micron diameter cylinder at 290 K. Empirical data give a drag coefficient (C_D) range between 20 and 13 for Re between 0.3 and 0.7 for flow over a cylinder.

The total number of fibers in the flow path is calculated as a function of porosity. The number of fibers varies linearly with porosity, so the pressure drop also varies linearly with porosity (pressure drop increases linearly with decreasing porosity). The drag force on one fiber is multiplied by the total number of fibers in the flow path to arrive at the total drag force. The total drag force is then divided by the cross-sectional flow area to calculate the pressure drop for a given porosity.

An alternative approach to estimating pressure drop in the high porosity regime of flow perpendicular to an array of rods uses a unit cell model developed by Happel [5]. The hydrodynamic permeability, κ, can be calculated using the following equation [4]:

$$\kappa = (a^2/8\alpha)\,(-\ln \alpha - 1.476)$$

where a is the fiber radius and α is the solid fraction. Darcy's Law can be used to calculate the one-dimensional pressure drop due to the fibrous media:

$$\Delta P = V\mu L_x/\kappa$$

The independent fiber model agrees with this theoretical model to within 15%.

Heat transfer calculation

The amount of heat transferred for a given porosity is calculated by modeling the fibers as individual pin fins:

$$h_{\substack{fiber \\ effective}} = \frac{\sqrt{h_{fiber} P k_{fiber} A_c}\,\tanh(mL)}{A_c}$$

where h_{fiber} is the heat transfer coefficient derived from the Nusselt number for flow over a cylinder at low Re:

$$h_{fiber} = \frac{\mathrm{Nu}\, k_{air}}{d_{fiber}}$$

The parameter m and the Nusselt number [3] are given by:

$$m = \sqrt{\frac{4h_{fiber}}{k_{fiber}\, d_{fiber}}}$$

$$Nu = 0.3 + \frac{0.62\mathrm{Re}^{\frac{1}{2}}\,\mathrm{Pr}^{\frac{1}{3}}}{\left[1 + \left(\frac{0.4}{\mathrm{Pr}}\right)^{\frac{2}{3}}\right]^{\frac{1}{4}}}$$

The perimeter of the fiber is P, thermal conductivity is k_{fiber}, cross-sectional area is A_c, and fiber length is L.

A unit cell is defined such that each fiber is contained in a patch of area that will decrease with decreasing porosity (assuming fiber diameter remains constant). The test article is treated as a counter-flow heat exchanger and an overall heat transfer coefficient is determined. We consider heat transfer via the fibers (modeled as pin fins in the above equations) and heat transfer via laminar flow at the walls in both hot and cold streams. Conduction through the aluminum backing and the effect of the carbon fiber-aluminum interface (provided by a conductive glue) were considered. Both were negligible and therefore neglected in calculating the overall heat transfer coefficient, U.

4.2.4 Modeling of metallic wools

The test article for metal wool has the same geometry as the 100% porous case. The hot stream flows through a cylindrical duct 5.1 cm in diameter. The cold stream is an annular region outside the hot stream duct that has an inner diameter of 5.1 cm and an outer diameter of 7.7 cm. The interface between the hot and cold streams is a thin sheet of aluminum.

Pressure drop calculation

The pressure drop prediction for the steel wool test article was calculated using a modified Ergun equation for circular cross-section fibers [6]:

$$\Delta P = \frac{8.22\rho(1-\phi)V^2}{1.5\phi^3 D_{fiber}} + \frac{193.8\mu(1-\phi)^2 V}{1.5\phi^3 D_{fiber}^2}$$

where φ = porosity. The fluid properties are for air at 300 K and the porosity is 99.8%. A fiber diameter of 300 microns was used.

Heat transfer calculation

A 2D porous media flow model called MERLOT (**M**odel of **E**nergy-transfer **R**ate for f**L**ow in **O**pen-porosity **T**ailored-media) was developed and used to determine the heat transfer coefficient for random porous media [7]. MERLOT uses the modified Darcy equation to evaluate the velocity distribution based on the local microstructure characteristics and pressure gradient, and uses the energy equation to calculate the temperature distribution and to evaluate the heat transfer performance of the porous medium. Key capabilities include:

* Accounting for a wide range of porosity variation by adjusting the porous medium properties accordingly (such as permeability);
* Modeling of the effect of dispersion based on the porous medium microstructure, which enhances the effective gas thermal conductivity;
* Accounting for non-isotropic properties, such as differing solid thermal conductivity values parallel and perpendicular to the flow (e.g. as in the case of fibrous media perpendicular to the flow)
* Accounting for variable heat transfer coefficient between gas and solid in the bulk based on the local flow and solid microstructure characteristics
* Inclusion of temperature-dependent effect of properties (in particular of solid and gas thermal conductivities).

Appendix A provides a brief description of the model.

For steel wool with assumed thermal conductivity of 25 W/m-K and porosity of 99.8%, MERLOT predicts h = 38 W/m^2-K at the 20 CFM flow rate. Predicted effectiveness for the steel wool is 6.1%. The MERLOT prediction of h for copper with the same fiber cross-section as the steel wool is h = 177 W/m^2-K. The copper has a predicted effectiveness of 23.5%. A summary of modeling results is given in Table 6.

Table 6. Summary of modeling of metallic wools (for L=25 cm)

porous material	porosity	thermal conductivity [W/m-K]	predicted *h* [W/m^2-K]	predicted ε
none	100%	N/A	20	4.1%
steel	99.8%	25	38	6.1%
copper	99.8%	400	177	23.5%

4.2.5 Parametric studies for carbon velvet

The use of a structured porous medium allows us to tailor several parameters in order to optimize the thermal-hydraulic performance. We examined carbon velvet with nominal parameters and then varied the porosity, fluid velocity, fiber conductivity and diameter in order to determine the impact on the heat exchanger effectiveness. The reference case around which we performed these parametric studies has 99.5% porosity, 1 m/s fluid velocity, 100 W/m-K conductivity and , and 6 μm, fiber diameter. In all cases, the length was fixed at 7 cm (the effectiveness and length are interdependent). The heat exchanger (test article) flow channels are coaxial annuli 5 mm wide between standard 2" and 3" coaxial pipes.

Figure 3 shows the variation with porosity. The effectiveness is monotonically decreasing, with the most rapid decrease occurring above 99%. From a practical point of view, higher porosity is desired in order to maintain a reasonable heat exchanger length. Using the nominal parameters shown above, a porosity of 98-99% appears optimal.

Figure 4 shows the variation with velocity. The effectiveness is monotonically decreasing with velocity, with no apparent minimum. This can be understood in terms of the definition of effectiveness:

$$\varepsilon = \frac{UPL}{UPL + \dot{m}c_p}$$

Since the overall heat transfer coefficient, U, varies more slowly with velocity than the energy throughput, slower velocities always improve the effectiveness. In order to achieve the desired ventilation rate, larger flow area is preferred over faster flow speeds.

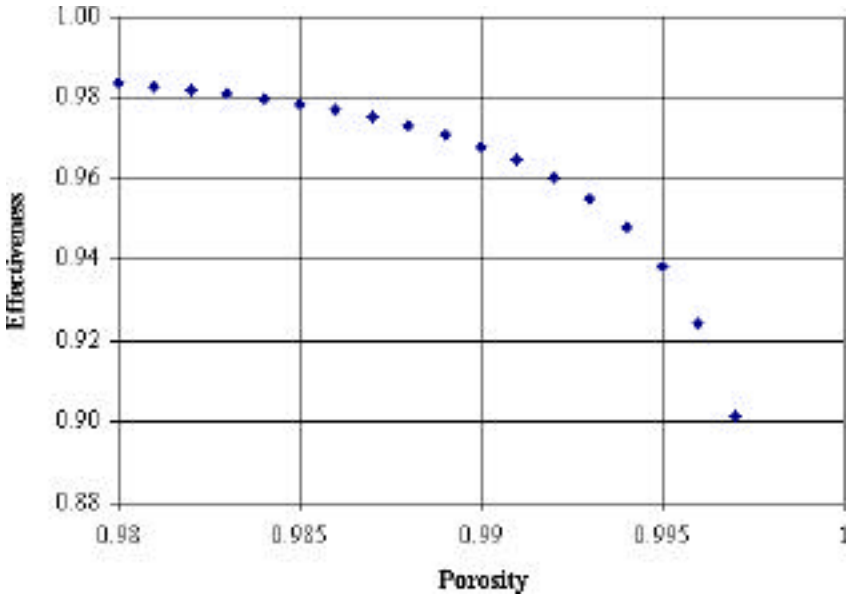

Figure 3. Variation of effectiveness with porosity

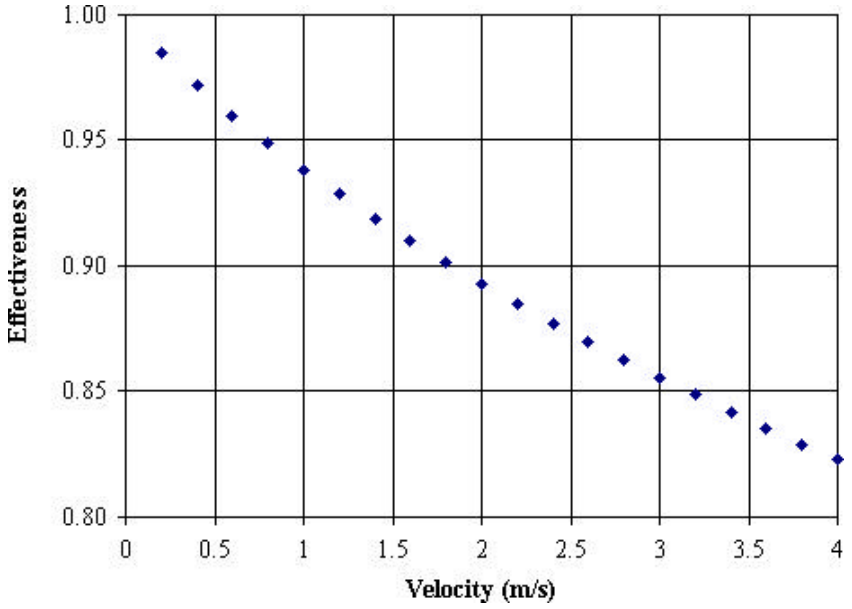

Figure 4. Variation of effectiveness with velocity

Figure 5 shows the variation with fiber conductivity. Obviously, higher conductivity is always better. Interestingly, diminishing returns occur above about 200 W/m-K. This value is relatively easy to obtain with several materials, including carbon, copper and aluminum.

Figure 6 shows the variation of effectiveness with fiber diameter. In order to achieve an effectiveness greater than 90%, a diameter smaller than 10 μm is needed (assuming 100 W/m-K conductivity). Smaller diameters are always better. However, smaller diameters also result in larger pressure drops with constant porosity.

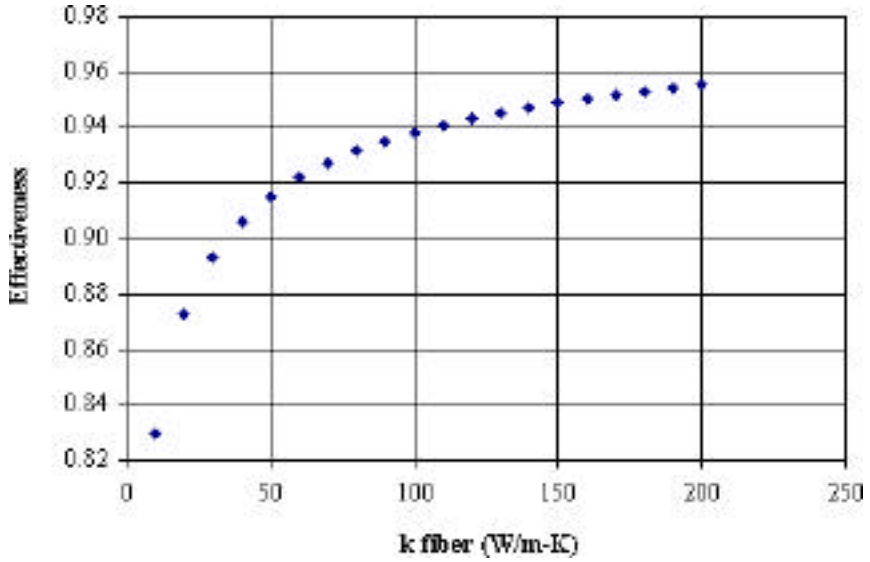

Figure 5. Variation of effectiveness with conductivity

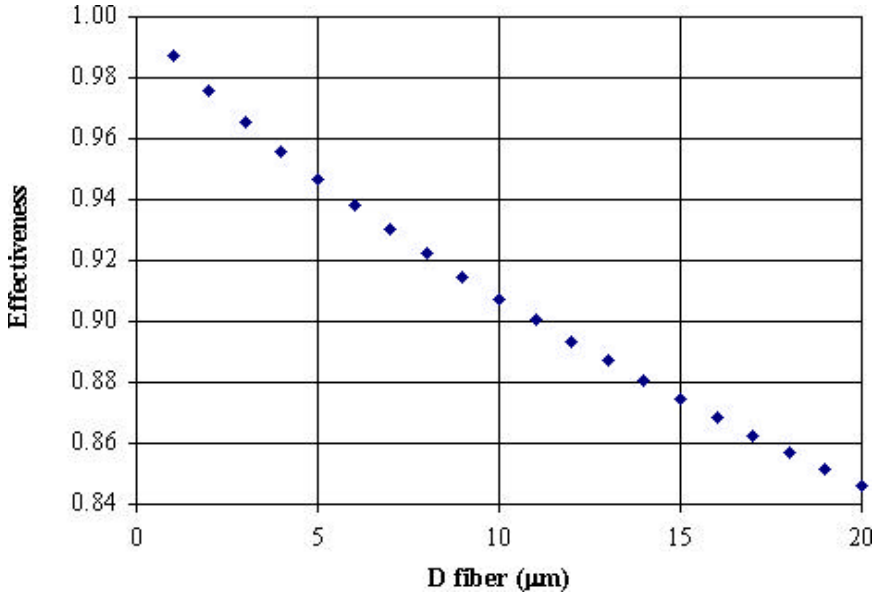

Figure 6. Variation of effectiveness with fiber diameter

Effectiveness is not the only parameter which governs the performance of an energy recovery ventilator. If the pumping power becomes a substantial fraction of the thermal power recovered, then the net efficiency of the device is compromised. A pumping power fraction of 5-10% of the thermal power recovered is a reasonable goal. Figures 7 and 8 show the pumping power fraction as a function of the fiber diameter and porosity. A diameter of 6 μm is at the lower end of the acceptable range; a value above 10 μm is probably more desirable. For this range of diameter, a porosity above 99% is needed to maintain acceptable pumping power.

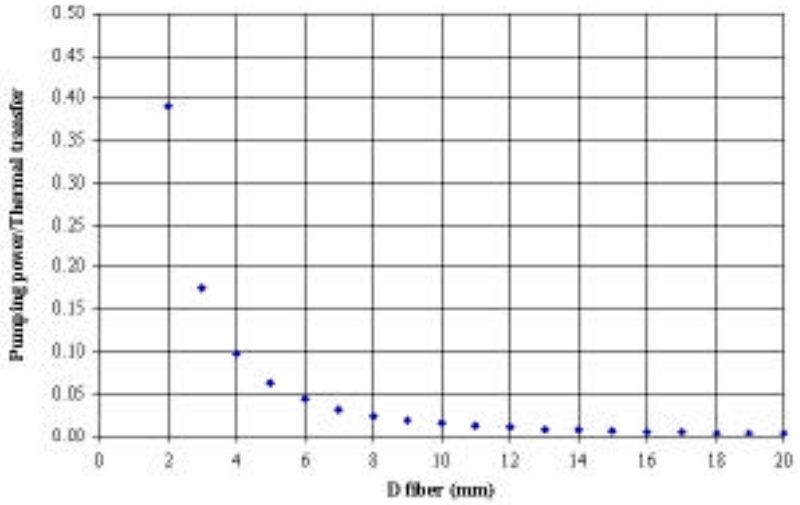

Figure 7. Variation of pumping power ratio with fiber diameter

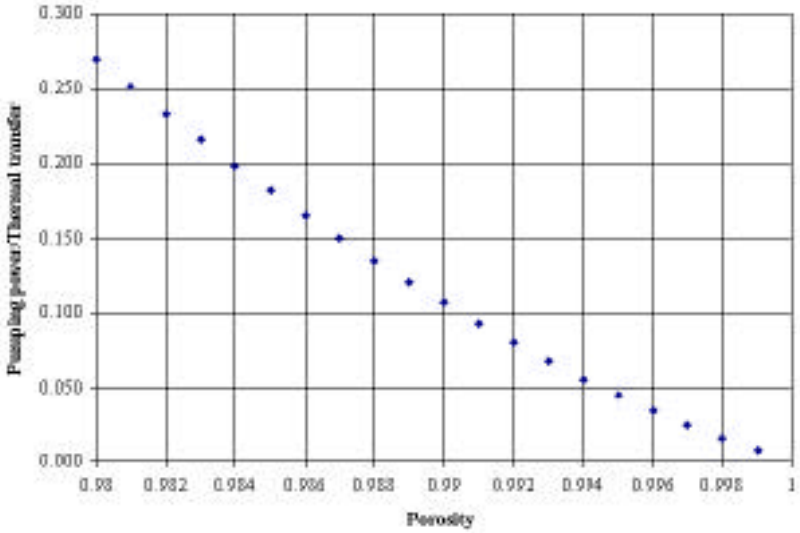

Figure 8. Variation of pumping power ratio with porosity

4.3 Experimental verification

Outcome: *Experiments were performed on open channels, metal wools and carbon velvet. Effectiveness in open channels agreed well with predictions, but the performance with porous media in the channels were consistently lower than expected. Flow bypass was a recurring problem, especially at higher velocities. Local and/or global flow redistribution could reduce both the pressure drop and heat transfer coefficient, consistent with observations. Measurements of the ratio of pumping power to thermal power removed actually agree reasonably well with predictions, supporting these observations.*

Testing was performed on porous metal and carbon heat exchangers using the experimental apparatus depicted in Figure 9. The main elements include the vertical concentric flow channels, blowers on the primary and secondary side of the heat exchanger, the primary heater, heater controller, SCXI signal conditioning module, and the computer data acquisition system. The flow loop was designed to accept a standard fitting, such that test articles could be easily inter-changed.

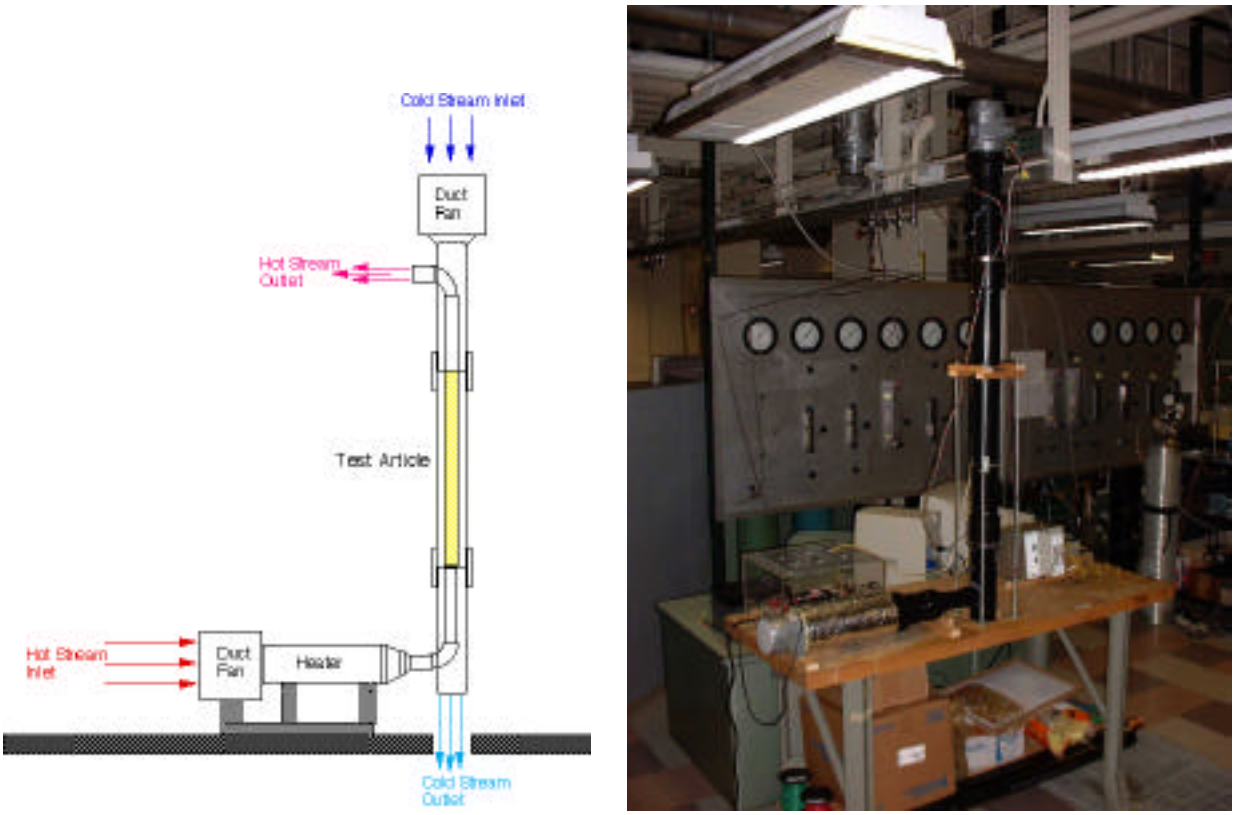

Figure 9. Process flow loop

Three cases were explored experimentally: (1) an open channel reference case, (2) carbon velvet, and (3) metal wools. All experiments used a fixed hot stream inlet temperature of 100 ˚F and a cold stream inlet temperature ranging between 74 and 77 ˚F (room temperature).

4.3.1 Open channel reference case

For the purpose of initial shakedown testing and to provide a benchmark for comparison, an open annulus was tested without porous media with air flow of 20 CFM in both streams. The predicted effectiveness was 4.1% using *h* predicted by Dittus-Boelter and the *Ntu* model presented in Section 4.2. The measured effectiveness was 4.2%. The total amount of heat available at 20 CFM flow is 145 Watts. Therefore, 4.2% of 145 Watts (6 Watts), is transferred by the 100% porous test article (see Table 7).

Table 7. Heat transfer results for the 100% porous test article (L = 25cm)

Flow (CFM)	$T_{H,in}$ (^{0}F)	$T_{C,in}$ (^{0}F)	$T_{C,out}$ (^{0}F)	Predicted ε (%)	Measured ε (%)
20	100	76	77	4.1	4.2

4.3.2 Carbon velvet

Energy Science Laboratories (ESLI) provided low-cost carbon fiber velvet for testing. The material has a porosity between 99.55% and 99.60%. Two test articles were fabricated – one with 25 cm length and one with 7 cm length – using standard 2 inch and 3 inch coaxial plastic pipes with two annular channels 5 mm wide. ESLI fibers are flocked on both sides of a thin aluminum sheet which is formed into a cylinder and inserted in the annular region between the two coaxial plastic pipes, thus forming the two 5 mm wide annular regions. Figure 10 shows a picture of the test article and Figure 11 shows a picture of individual fibers.

The 25-cm test article was run initially with a flow rate of 7 CFM in both streams (velocity of approximately 3.5 m/s). The measured heat exchanger effectiveness was 75.8% for this initial test. For these flow rates, >90% effectiveness should have been obtained based on the independent fiber model. The pressure drop was measured in order to determine whether flow

bypass might be causing the reduced effectiveness. The inner stream pressure drop was 1,250 Pa (5 in-H_2O), while the outer stream pressure drop was 4,600 Pa (18 in-H_2O). The expected pressure drop is about 5,000 Pa (20 in-H_2O), so it appears that flow was bypassing the fibers in the inner flow stream. This is believed to be the reason that the effectiveness was less than expected in this initial test.

Figure 10. Carbon fiber and metal wool test articles

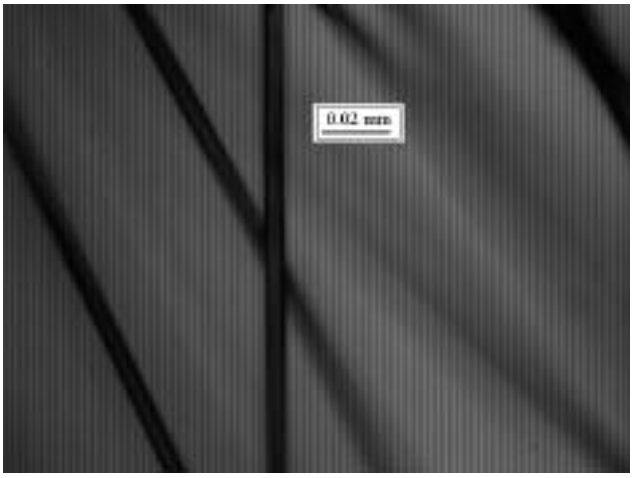

Figure 11. Magnified view of carbon fibers

The 25-cm test article was repaired and tested again. The flow rate was reduced to 3.3 CFM due to flow limitations on the air supply. The measured heat exchanger effectiveness in this case was 77%. The pressure drop at this flow rate was 9.9 in-H_2O and 9.8 in-H_2O in the hot and cold streams, respectively.

In order to attain pressure drop measurements over a broader range of flow, a 7-cm test article was fabricated and tested. The measured heat exchanger effectiveness for this test article was 53% for a flow rate of 3.3 CFM in both streams, as compared with 88.5% predicted by theory. Table 8 summarizes the experimental and theoretical heat transfer results for the two test articles. The predicted effectiveness of the 7 cm test article was 88.5% using the independent fiber model, while the predicted effectiveness for the 25 cm test article was 96.5%. The actual effectiveness of each test article is significantly less than the independent fiber model predicts.

Table 8. Heat transfer results for ESLI test articles

L (cm)	Flow (CFM)	$T_{H,in}$ (^{0}F)	$T_{H,out}$ (^{0}F)	$T_{C,in}$ (^{0}F)	Predicted ε (%)	Measured ε (%)
7	3.3	100	88	77.5	88.5	53
25	3.3	100	83	78	96.5	77

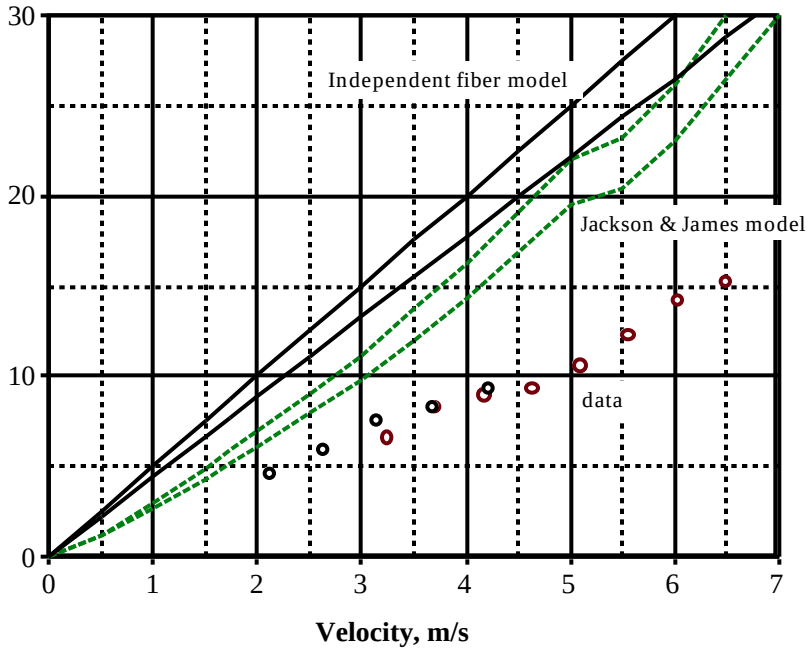

Figure 12. Pressure drop predictions and experimental data for ESLI test articles

Pressure drop results are shown in Figure 12. The theoretical predictions from the Jackson and James model and the independent fiber model for the pressure drop are also shown. The fact that the data indicates a lower pressure drop than expected tends to suggest that some amount of flow bypass is still present, which could explain the lower than expected thermal performance.

Table 9 compares the thermal power transferred to the pumping power required for ventilation. Results are for a 22^0F temperature difference between $T_{H,in}$ and $T_{C,in}$ as shown in Table 8. Therefore, the maximum possible thermal power transferred is 22 W. Theoretical effectiveness and pressure drop calculations are based on 6-μm diameter fibers and thermal conductivity of 100 W/m-K. Both the pumping power and the thermal power are lower than expected, indicating a consistent discrepancy. The ratio of pumping power to thermal power agrees better, especially with the shorter test article. We believe this is due to flow redistribution which allows part of the flow to avoid some fibers.

Table 9. Pumping power *vs.* thermal power recovered for the ESLI heat transfer medium

	length (cm)	effectiveness	thermal power (W)	pumping power (W) (indep. fiber model)	PP/TP
theory	7	88.5%	19.5	2.3	11.8%
	25	96.5%	21.2	8.2	38.7%
experiment	7	53%	11.7	1.4 (extrapolated)	12.0%
	25	77%	16.9	3.9	23.1%

4.3.3 Metal wools

A 25 cm long test article was constructed for use with various randomly oriented metal wool materials (see Figure 10 and 13). It consists of a coaxial exchanger with an outer annular region 1.5 cm wide and an inner circular region with a diameter of 5 cm. The two streams are separated by the same type of aluminum foil used in the ESLI fiber test article.

The empty coaxial test article was filled with steel wool at 99.8% porosity and tested at 17 CFM (maximum available flow for the fans with the porous media obstruction). Copper wools were more difficult to pack uniformly, so measurements were taken using steel wool.

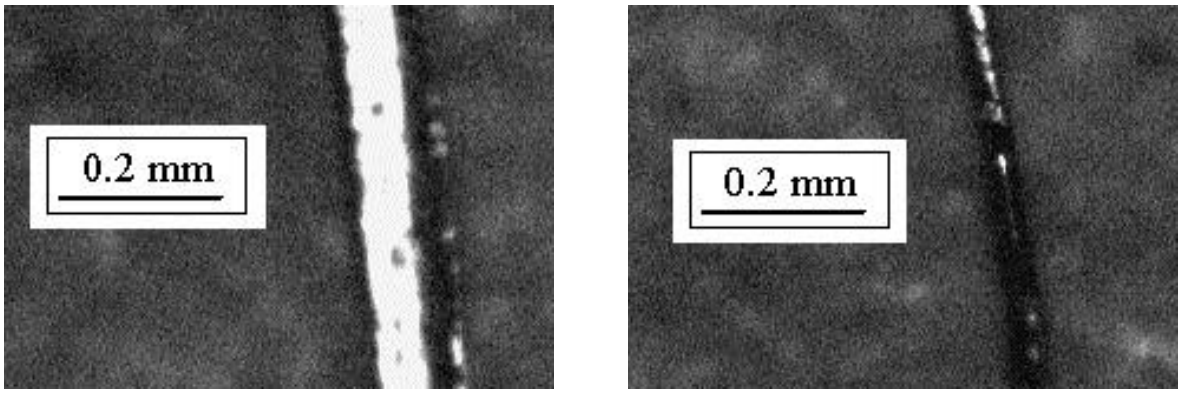

Figure 13. Magnified view of ribbon-like metal wool fibers (a. broad side, b. narrow side)

Pressure drop data are compared with model predictions in Figure 14 and the measured and predicted effectiveness are summarized in Table 10. As seen with the ESLI velvet, the measured values are consistently lower than the predicted values.

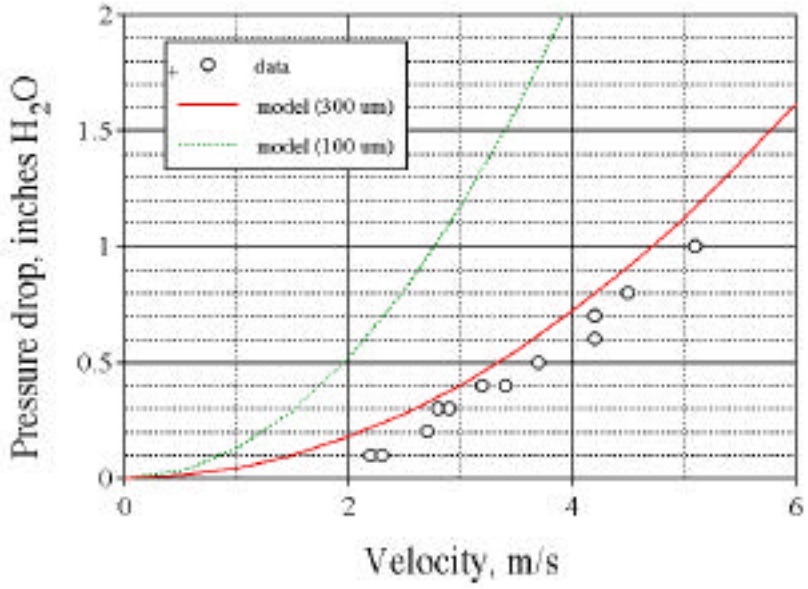

Figure 14. Pressure drop data and model predictions using the modified Ergun equation for 100 μm and 300 μm diameter fibers

Table 10. Heat transfer results for the steel wool test article

Flow rate (CFM)	$T_{H,in}$ (^{0}F)	$T_{C,in}$ (^{0}F)	$T_{C,out}$ (^{0}F)	Predicted ε (%)	Measured ε (%)
17	100	77	79	6.1	8.7

5. Conclusions and Recommendations

Numerical modeling indicates that the optimum performance of porous media heat exchangers occurs with fiber diameters above about 10 μm and porosity in the range of 98-99%. In this range, effectiveness over 90% is predicted while maintaining pumping power within reasonable limits. Both random and oriented fiber geometries appear to offer adequate performance. Experimental studies were unable to replicate the high performance predicted by numerical modeling. Since both pressure drop and heat transfer coefficient were depressed, the most likely explanation for the discrepancies is the existence of flow bypass.

Two primary improvements are recommended in order to further explore the potential of carbon velvet porous media. First, extensive parametric studies indicated that the choice of parameters for the materials used in the experiments were not optimum. In order to achieve higher effectiveness, slightly larger fiber diameters with porosity of 99% (instead of 99.5%) should be used. In addition, fibers with conductivity about a factor of two higher (200 W/m-K), which is relatively straightforward and carries little cost penalty, should be used. Second, greater care should be taken to assure that the fibers are well attached to the walls in order to prevent flow bypass. This is actually rather simple to do by interlocking velvets which are bonded to both sides of the coolant channels.

Model predictions suggest that metallic wools could offer equal or better performance as compared with carbon velvets if sufficiently high conductivity materials, such as copper, could be obtained with appropriate dimensions and packing characteristics. Further exploration of low-cost sources of high-porosity, high-conductivity metal fillers is needed.

6. Public Benefits to California

The cost of installing an energy recovery ventilator system may or may not offset the energy savings, depending on many factors. The price of existing ERV's ranges from $500 to over $2000. Therefore, an energy savings of at least $50–100 per year is an important goal. Depending on local climate, appliance use, and sealing method, tighter houses can be 15–30% more energy efficient than their older counterparts, offering potential savings of hundreds of dollars per household in annual energy costs. However, in less optimal situations and considering the low thermal efficiency of existing units, the savings may be much lower. Clearly, widespread implementation of these energy-saving devices depends on optimized system performance.

Successful development of high-effectiveness heat exchangers will expedite the application of energy recovery ventilators in California. For a well-sealed house, assuming an electricity cost of $0.10/kWh, an energy recovery ventilation system with a 90% effectiveness and a duty factor of about 45% would result in a utility cost saving of about $400 per year.

Development Stage Assessment

The objective of this research was to develop a better understanding of the limitation of high-conductivity porous media for enhancing the effectiveness of energy recovery ventilators. Modeling performed to help optimize the material architecture and experiments were performed to determine whether or not the actual heat exchanger performance would meet expectations. This activity falls primarily under the "Engineering/Technical" activity. In the performance of the research, some initial ideas were generated on the end market, product development and public benefits. However, these were not the primary motivation of the research.

Development Assessment Matrix

Stages / Activity	1 Idea Generation	2 Technical & Market Analysis	3 Research	4 Technology Develop-ment	5 Product Develop-ment	6 Demon-stration	7 Market Transfor-mation	8 Commer-cialization
Marketing								
Engineering / Technical								
Legal/ Contractual								
Risk Assess/ Quality Plans								
Strategic								
Production. Readiness/								
Public Benefits/ Cost								

Nomenclature and Glossary

c_p	heat capacity
d	inner (hot stream) pipe diameter
h	heat transfer coefficient
k_{fiber}	fiber conductivity
$\dot{m}$	mass flow rate
q_{max}	maximum heat flux
t	thickness of conductive wall between streams
ACH	air changes per hour
C	flow thermal capacity [J/K s]
CFM	cubic feet per minute
C_D	drag coefficient
D	outer diameter of cold stream annulus
D_{fiber}	fiber diameter
F	drag force on a fiber
L	fiber length
L_x	length of the heat exchanger
NTU	number of transfer units
P	fiber perimeter
Q	heat transferred
Re_d	Reynolds number (based on d)
T_{in}	hot stream inlet temperature
T_{out}	hot stream outlet temperature
U	overall heat transfer coefficient
V	flow velocity
W	volume flow rate
α	solid fraction
ε	effectiveness
φ	porosity
κ	hydrodynamic permeability
μ	dynamic viscosity [kg/m-s]
ρ	fluid density [kg/m^3]
ΔP	total pressure drop

References

[1] US Department of Energy Reference Brief, Energy Efficiency and Renewable Energy Clearinghouse (http://www.eren.doe.gov/consumerinfo/refbriefs/ea5.html).

[2] M. Drost, “Air-to-Air Heat Exchanger Performance,” Energy and Buildings **19** (3) pp. 215-220, 1993.

[3] S. W. Churchill and M. Bernstein, “A Correlating Equation for Forced Convection from Gases and Liquids to a Circular Cylinder in Crossflow,” *J. Heat Trans.* **99** (1977) 300-306.

[4] G. W. Jackson and D. F. James, “The Permeability of Fibrous Porous Media”, *Can. J. Chem. Eng.* **64** (1986) 364-374.

[5] Happel, J., 1959, “Viscous Flow Relative to Arrays of Cylinders”, *AIChE J.* **5**, 174-177.

[6] Macdonald, *et al.*, “Flow Through Porous Media – The Ergun Equation Revisited”, Ind. Eng. Chem. Fundam. **18** (3) 1979.

[7] A. R. Raffray and J. E. Pulsifer, "MERLOT: A Model for Flow and Heat Transfer through Porous Media for High Heat Flux Applications," UCSD-ENG-087, November 2001.

Appendix A. Description of MERLOT

To help in analyzing and optimizing advanced heat transfer media, a 2D porous media flow model called MERLOT **(M**odel of **E**nergy-transfer **R**ate for f**L**ow in **O**pen-porosity **T**ailored-media) was developed and adapted for this activity [A1]. It uses the modified Darcy equation to evaluate the velocity distribution based on the local microstructure characteristics and pressure gradient, and uses the energy equation to calculate the temperature distribution and to evaluate the heat transfer performance of the porous medium.

First, the continuity equation and the modified Darcy equation including Forcheimer's drag term and Brinkman's viscosity term are used in estimating the velocity profile [A2]. For fully-developed steady state flow though a 2-D cylindrical geometry (r,θ) such as shown in Fig. 3, these can be expressed as:

$$\frac{\partial V_\theta}{\partial \theta} = 0 \tag{3}$$

$$0 = -\frac{1}{r}\frac{\partial P}{\partial \theta} - \left(\frac{\mu}{K}\right)V_\theta - \left(\frac{\rho_f C}{\sqrt{K}}\right)V_\theta^2 + \mu_{eff}\frac{\partial}{\partial r}\left(\frac{1}{r}\frac{\partial}{\partial r}(rV_\theta)\right) \tag{4}$$

where V_θ is the superficial velocity in the θ direction, P the fluid pressure μ the fluid viscosity; K the porous medium permeability, ρ_f the fluid density, and C the inertia coefficient.

Eq. (4) can be non-dimensionalized as follows, where the primes refer to non-dimensionalized variables and V_{θ_0} and P_o are the reference Darcy velocity and pressure, respectively.

$$r' = \frac{r}{r_{out}} \tag{5}$$

$$V'_\theta = \frac{V_\theta}{V_{\theta_0}} \tag{6}$$

$$P' = \frac{P - P_0}{\rho_f V_{\theta_0}^2} \tag{7}$$

$$0 = -\frac{1}{r'}\frac{\partial P'}{\partial \theta} - \frac{V'_\theta}{\mathrm{Re}_{ch}\,Da} - \left(\frac{CV'^2_\theta}{\sqrt{Da}}\right) + \frac{1}{\mathrm{Re}_{ch}}\frac{\partial}{\partial r'}\left(\frac{1}{r'}\frac{\partial}{\partial r'}(r'V'_\theta)\right) \tag{8}$$

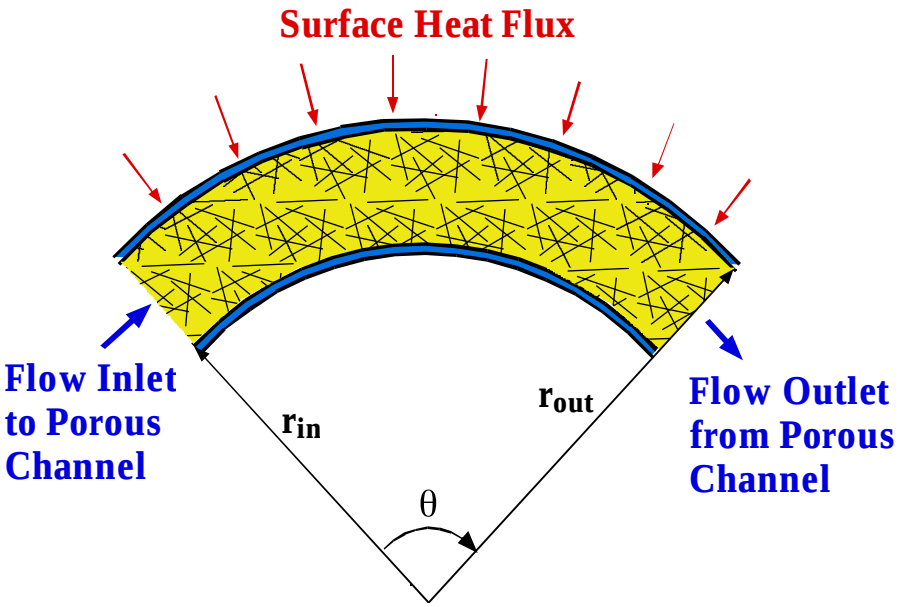

Figure A1. Model geometry for flow through porous media

where the Darcy number, *Da,* and Reynolds number for the channel, Re_{ch} are defined as:

$$Da = \frac{K}{r_{out}^2} \qquad (9)$$

$$\mathrm{Re}_{ch} = \frac{\rho_f V_{\theta 0} r_{out}}{\mu_{eff}} \qquad (10)$$

An implicit finite difference scheme is used to solve Eq. (8) in combination with a tri-diagonal matrix solver subroutine using the Thomas algorithm [A3]. The non-dimensional pressure gradient is assumed constant and set as input and the boundary conditions are no slip at both walls (*i.e.*, $V'_{\theta,wall} = 0$). Due to the non-linear velocity term in Eq. (8), an iterative procedure is used to advance the solution by using the old value of velocity to compute the new ones until the desired convergence is reached.

Next, the 2-D temperature distribution can be obtained by separately solving the energy equations for the solid phase and the fluid phase, using a local heat transfer coefficient, h_c, at the interface between solid and fluid [A2]. The equations are expressed so as to include the effect of spatial variations of thermal conductivity and porosity.

$$0 = \frac{1}{r}\frac{\partial}{\partial r}(r(1-\phi)k_{s,r}\frac{\partial T_s}{\partial r}) + \frac{1}{r^2}\frac{\partial}{\partial \theta}((1-\phi)k_{s,\theta}\frac{\partial T_s}{\partial \theta}) + (1-\phi)q'''_s + h_c S_{BET}(T_f - T_s) \quad (11)$$

$$\rho_f Cp_f \frac{V_\theta}{r}\frac{\partial T_f}{\partial \theta} = \frac{1}{r}\frac{\partial}{\partial r}(r\phi k_{f,t,r}\frac{\partial T_f}{\partial r}) + \frac{1}{r^2}\frac{\partial}{\partial \theta}(\phi k_{f,t,\theta}\frac{\partial T_f}{\partial \theta}) + \phi q'''_f + h_c S_{BET}(T_s - T_f) \quad (12)$$

where ϕ is the porosity; $k_{s,r}$ and $k_{s,\theta}$ the solid thermal conductivities in the r and θ direction, respectively; T_s and T_f the solid and fluid temperatures, respectively; q'''_s and q'''_f the volumetric heat generations in the solid and fluid, respectively; S_{BET} the specific surface area of the porous medium; ρ_f the fluid density; Cp_f the fluid heat capacity; and $k_{f,t,r}$ and $k_{f,t,\theta}$ the total effective fluid thermal conductivities in the r and θ direction, respectively.

$k_{f,t,r}$ and $k_{f,t,\theta}$ include the fluid thermal conductivity itself (k_f) and the enhancement provided by dispersion effects ($k_{disp,r}$ and $k_{disp,\theta}$) [A4].

$$k_{f,t,r} = k_f + k_{disp,r};\ k_{f,t,\theta} = k_f + k_{disp,\theta} \quad (13)$$

Eqs. (11) and (12) can be non-dimensionalized as follows, where again the primes refer to non-dimensionalized variables and T_h and T_c refer to the cold and hot reference temperatures, respectively. The property data and the heat generation values are all non-dimensionalized by using reference values (denoted with the subscript *ref*).

$$T'_s = \frac{T_s - T_c}{T_h - T_c};\ T'_f = \frac{T_f - T_c}{T_h - T_c} \quad (14)$$

$$k'_s = \frac{k_s}{k_{s,ref}};\ k'_f = \frac{k_f}{k_{f,ref}} \quad (15)$$

$$\rho'_f = \frac{\rho_f}{\rho_{f,ref}} \quad (16)$$

$$Cp'_f = \frac{Cp_f}{Cp_{f,ref}} \quad (17)$$

$$q'_s = \frac{q'''_s}{q'''_{ref}};\ q'_f = \frac{q'''_f}{q'''_{ref}} \quad (18)$$

$$h'_{eff} = \frac{h_c S_{BET}(T_h - T_c)}{q'''_{ref}} \tag{19}$$

The following parameters, J_s, $J_{f,1}$ and $J_{f,2}$ are introduced to simplify the equation display:

$$J_s = \frac{k_{s,ref}(T_h - T_c)}{r_{out}^2} \tag{20}$$

$$J_{f,1} = \frac{k_{f,ref}(T_h - T_c)}{r_{out}^2} \tag{21}$$

$$J_{f,2} = \frac{\rho_{f,ref} Cp_{f,ref} V_{\theta_0}(T_h - T_c)}{r_{out}} \tag{22}$$

$$0 = J_s\left(\frac{1}{r'}\frac{\partial}{\partial r'}\left(r' k'_{s,r}(1-\phi)\frac{\partial T'_s}{\partial r'}\right) + \frac{1}{r'^2}\frac{\partial}{\partial \theta}\left(k'_{s,\theta}(1-\phi)\frac{\partial T'_s}{\partial \theta}\right)\right) + (1-\phi)q''_{ref}\, q''_s + q''_{ref}\, h'_{eff}(T'_f - T'_s) \tag{23}$$

$$J_{f,2}\rho'_f Cp'_f \frac{V'_\theta}{r'}\frac{\partial T'_f}{\partial \theta} = J_f\left(\frac{1}{r'}\frac{\partial}{\partial r'}\left(r' k'_{f,t,r}\phi\frac{\partial T'_f}{\partial r'}\right) + \frac{1}{r'^2}\frac{\partial}{\partial \theta}\left(k'_{f,t,\theta}\phi\frac{\partial T'_f}{\partial \theta}\right)\right) + \phi q''_{ref}\, q''_f + q''_{ref}\, h'_{eff}(T'_s - T'_f) \tag{24}$$

Although the above equations are expressed in general terms to include the effect of porosity variation in both r and θ directions, in the geometry of interest represented in Fig. 1, the porosity will only vary with r but not with θ.

Eqs. (23) and (24) are solved based on an implicit alternating direction finite difference scheme using the velocity distribution from the solution of Eq. (8) as input and based on the following boundary conditions [A3]:

- At inlet, $\theta = 0$, the temperature is set at the uniform inlet temperature; and
- At outlet, $\theta = \theta_{out}$ for simplicity, adiabatic conditions are assumed.
- At both walls, $r=r_{in}$ and $r=r_{out}$, the boundary conditions are set by equating the total heat flux, q''_w to the combined fluid and solid heat fluxes. For example, for the inner wall the boundary condition is:

$$(q''_w = -(1-\phi)k_{s,r}\frac{\partial T_s}{\partial r} - \phi k_{f,t,1}\frac{\partial T_f}{\partial r})_{innerwall} \tag{25}$$

$k_{f,t1}$ in the equation represents an effective conductivity for the fluid at the wall including a convection component averaged over the radial increment at the wall.

Eq. (25) can be written in non-dimensional form as follows:

$$(q'_w q''_{w,ref} = -\frac{(T_h - T_c)}{r_{out}}((1-\phi)k_{s,ref}k'_{s,r}\frac{\partial T'_s}{\partial r'} - \phi k_{f,ref}k'_{f,t,1}\frac{\partial T'_f}{\partial r'})_{innerwall} \quad (26)$$

where the wall heat flux is non-dimensionalized based on a reference value:

$$q'_w = \frac{q''_w}{q''_{w,ref}} \quad (27)$$

The solution proceeds iteratively. First, tri-diagonal matrix equations for the temperature in the r direction along each successive theta plane are solved using the old temperature values in the theta direction terms. Next, similar tri-diagonal matrix equations but for the temperature along the theta direction are solved using the just computed temperature values in the r-direction. The program iterates in these alternating direction solutions until the desired convergence is achieved.

References for Appendix A

A1. A. R. Raffray and J. E. Pulsifer, "MERLOT: A Model for Flow and Heat Transfer through Porous Media for High Heat Flux Applications," UCSD-ENG-087, November 2001.

A2. D. A. Nield and A. Bejan, “Convection in Porous Media,”2nd edition, Springer, New York, 1999.

A3. D. A. Anderson, J. C. Tannehill and R. H. Pletcher, “Computational Fluid Mechanics and Heat Transfer,” Hemisphere Publishing Corporation, New York, 1984.

A4. C. T. Hsu and P. Cheng, “Thermal Dispersion in Porous Medium,” Int. J. Heat Mass Transfer, Vol. 33, No. 8, pp1587-1597, 1990.